대한기계학회 2000년도 추계학술대회논문집 A pp. 665~670 KSME 00F096

Dynamic Instability of a Disc Brake Pad under Distributed Friction Forces

Boo-Jin Oh*, Bong-Jo Ryu**, Kyung-Bin Yim***,
Yoshihiko Sugiyama**** and Si-Ung Ryu****

분포마찰력을 받는 디스크 브레이크 패드의 동적 불안정

오부진, 류봉조, 임경빈, 杉山吉彦, 류시웅

Key Words: Dynamic Instability(동적 불안정), Disc Brake Pad(디스크 브레이크 패드), Distributed Friction Force(분포마찰력), Finite Element Method(유한요소법)

Abstract

The paper presents the dynamic instability of a disc brake pad subjected to distributed friction forces. A brake pad can be modeled as a beam with two translational springs. The study of this prototypical model is intended to provide a fundamental understanding of disc brake pad instabilities. Governing equations of motion are derived form energy expressions and their corresponding solutions are obtained by employing the finite element method.

The critical distributed friction force and the instability regions are demonstrated by changing two translational spring constants. Finally, the changes of eigen-frequencies of a beam determining instability types are investigated for various combinations of two spring constants.

1. Introduction

The brake is a mechanical device that produces the braking forces using dry friction. The noise generated in the brake system of cars is considered as an unstable vibration phenomenon due to friction forces. It has been an important technical task how to reduce the noise produced in the disc brake system that is widely employed in both airplanes and automobiles.

In general, the governing equation for the vibration of a disc bake pad under the excitation of a rotating disc is known to be basically the same as that for a beam model under distributed friction forces. Where, the distributed friction forces present the distributed follower forces in the tangential direction of a beam. These forces are obtained by multiplying the normal contacting force due to the brake pressure by the friction coefficient.

The dynamic stability problem on such a beam model with distributed follower forces has been studied as a nonconservative elastic stability problem by many investigators.[1-3]

Leipholz[4] presented both the dynamic stability and the critical distributed friction forces on a beam subjected to the distributed follower forces due to distributed friction forces for four different boundary conditions such as pin-pin, clamped-pin, clamped-clamped, and clamped-free conditions. He found that the flutter-type instability occurs for the clamped-free case while the divergence-type occurs for three other cases.

The study on the dynamic stability of a beam under distributed follower forces presented above does not intend to apply directly the disc brake pad.

* Member, Graduate School Student, Teajon National University of Technology
** Member, Faculty of Mechanical Engineering, Teajon National University of Technology
*** Dong-Yang Technical College
**** Osaka Prefecture University

However, the strip of pad has been treated in many studies as a beam with various boundary conditions since some experiments on the disc brake system showed that the brake pad and the associated boundary conditions have a great influence on the brake noise.[5-7]

Richmond and his colleagues[8] developed the computer program for the design of a disc brake pad. Hulten and Flint[9] studied the disc brake squeal using the assumed modes method.

Recently, Kang and Tan[10] used Galerkin´s method to investigate the dynamic stability of the Euler-Bernoulli beam by regarding the friction force acting on the brake pad as the pulsating distributed follower force. As presented above, the dynamic stability of a disc brake pad has been mostly studied by employing a beam model with conventional boundary conditions subjected to either uniformly or pulsating distributed friction forces.

In this paper, however, a beam with elastic supports are used since the brake parts such as caliper piston, caliper, and supporting bracket are regarded as translational springs. The dynamic stability of the beam under the uniformly distributed friction forces is studied using the finite element method.

2. Theoretical Analyses

2.1 Mathematical model

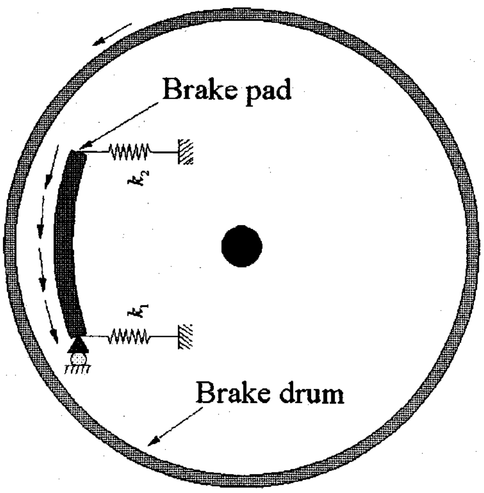

Fig. 1 Schematic diagram of disc brake and pad system.

The dynamic stability of a brake pad in the disc brake can be simply studied by modeling the disc brake system as a beam with spring supports at both ends subjected to the uniformly distributed follower forces.

Figure 1 is the schematic diagram of the disc brake system. Figure 2 depicts the simplified mathematical model of the system.

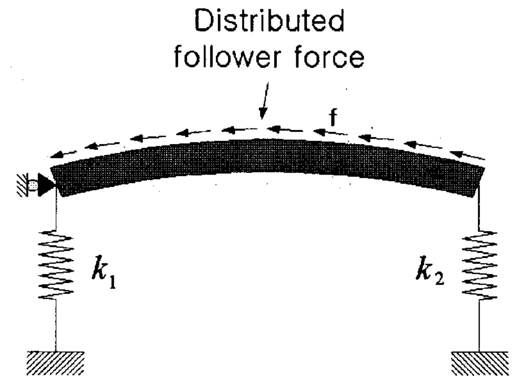

Fig. 2 A Mathematical model of an elastically restrained beam under distributed friction forces.

2.2 Energy expression

The equation of motion of the model shown in Figure 1 can be obtained from the following energy expression.

$$T=\frac{1}{2}\int_0^L(\rho A\, y_t^2)dx \tag{1}$$

$$V=\frac{1}{2}\int_0^L(EI\, y_{xx}^2)dx+\frac{1}{2}k_1 y^2(0,t)+\frac{1}{2}k_2\, y^2(L,t) \tag{2}$$

$$W_C=\frac{1}{2}\int_0^L f(L-x)\, y_x^2\, dx \tag{3}$$

$$\delta W_{NC}=-f\int_0^L y_x\, \delta y dx \tag{4}$$

Equation (1) represents the kinetic energy due to the translational movement of the beam. The first term of Equation (2) represents the potential energy of the beam due to bending, the second and the third terms represent the potential energy of the left and the right springs due to deflection, respectively.

Equations (3) and (4) represent the conservative work and the nonconservative virtual work done by the distributed friction forces, respectively. Where, subscripts x and t represent the differentiation with respect to position and time, respectively.

Substituting Equations (1)-(4) into the extended Hamilton's principle gives

$$\delta\int_{t_1}^{t_2}(T-V+W_C)+\int_{t_1}^{t_2}\delta W_{NC}\,dt=0 \qquad (5)$$

Separating variables and rearranging yields

$$\int_0^L[\rho A y_{tt}\delta y+EIy_{xx}\,\delta y_{xx}-f(L-x)y_x\delta y_x+fy_x\delta y]dx$$

$$+\ k_1 y(0,t)\delta y(0,t)+k_2 y(L,t)\delta(L,t)=0 \qquad (6)$$

2.3 Finite element model

Since it is not easy to find the exact solution of Equation (6), the beam is divided into N elements as shown in Figure 3 to obtain the discretized equations of Equation (6).

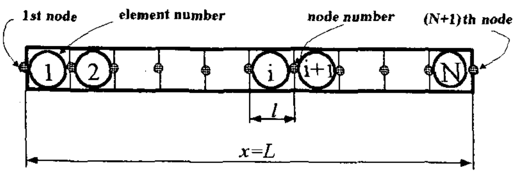

Fig. 3 A finite element model for considered system.

Introducing the following nondimensional coordinates for the calculation convenience

$$x'=x-(i-1)l,\quad \eta=\frac{y}{l},\quad \xi=\frac{x'}{l} \qquad (7)$$

gives

$$\sum_{i=1}^{N}\int_0^1[\rho Al^3\ \eta_{tt}^{(i)}\ \delta\eta^{(i)}+\frac{EI}{l}\ \eta_{\xi\xi}^{(i)}\ \delta\eta_{\xi\xi}^{(i)}-fl^2\{(N-$$

$$(\xi+i-1))\ \eta_\xi^{(i)}\ \delta\eta_\xi^{(i)}-\eta_\xi^{(i)}\delta\eta^{(i)}\}]d\xi+k_1 l^2\eta(0,t)^{(1)}$$

$$\delta\eta(0,t)^{(1)}+k_2 l^2\eta(1,t)^{(N)}\ \delta\eta(1,t)^{(N)}=0 \qquad (8)$$

Multiplying both sides of Equation (8) by EI/l and assuming the solution in the form of

$$\eta(\xi,t)=\eta(\xi)e^{i\omega t} \qquad (9)$$

yields

$$\sum_{i=1}^{N}\int_0^1\Big\{-\frac{\Omega^2}{N^4}\eta(\xi)^{(i)}\delta\eta(\xi)^{(i)}+\eta_{\xi\xi}(\xi)^{(i)}\delta\eta_{\xi\xi}(\xi)^{(i)}$$

$$-\frac{F}{N^3}\ \eta_\xi(\xi)^{(i)}\delta\eta_\xi(\xi)^{(i)}+\frac{F}{N^3}\ \eta_\xi^{(i)}\ \delta\eta_\xi^{(i)}\Big\}d\xi$$

$$+\frac{K_1}{N^3}\eta(0)^{(1)}\delta\eta(0)^{(1)}+\frac{K_2}{N^3}\eta(1)^{(N)}\delta\eta(1)^{(N)}=0 \quad (10)$$

where, the nondimensional parameters are

$$\Omega^2=\frac{\rho AL^4\omega^2}{EI},\quad F=\frac{fL^3}{EI},$$

$$K_1=\frac{k_1L^3}{EI},\qquad K_2=\frac{k_2L^3}{EI} \qquad (11)$$

In Equation (11), Ω is the frequency parameter, F is the distributed follower force parameter, K_1 and K_2 are the translational spring constant at left and right ends, respectively. Combining Equation (10) for N elements gives the following eigenvalue equation in matrix form.

$$\{[K]-\Omega^2[M]\}\{U\}=\{0\} \qquad (12)$$

3. Numerical Analyses and Results

Numerical analyses were performed based on the theoretical development presented above. In order to check the accuracy of numerical results obtained in the study, a comparison was conducted with the results in references[3] for the case of simply supported at both ends. The differences between two results are within 0.018% when 20 elements are used for the present study.

Figure 4 shows both the critical distributed friction force and the instability type for various right spring constants, K_2, when the left spring constant, K_1=1, 2, 5, 10, 12.

As shown in the figure, the critical distributed friction force increases as the spring constant K_1 increases. The transition of the instability type from a flutter to a divergence occurs as K_2 increases for each value of K_1.

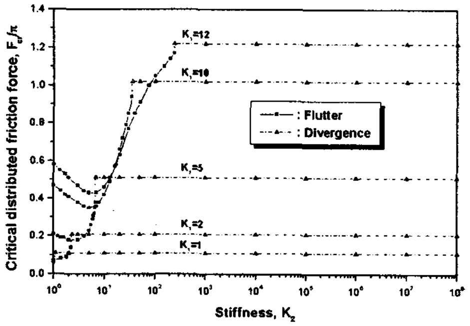

Fig. 4 Instability transitions depending on the spring stiffness (K_1 = 1, 2, 5, 10, 12 and K_2).

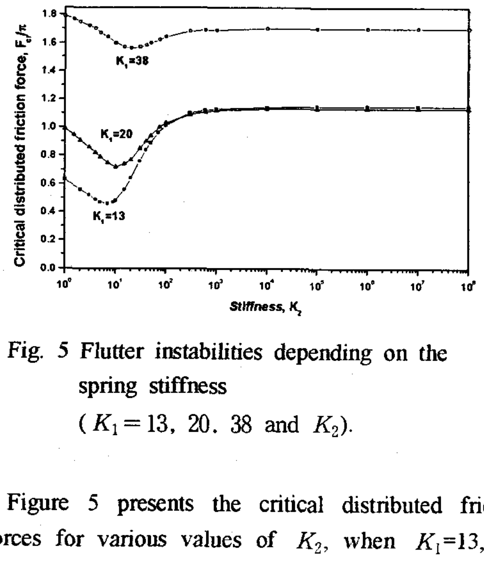

Fig. 5 Flutter instabilities depending on the spring stiffness (K_1 = 13, 20, 38 and K_2).

Figure 5 presents the critical distributed friction forces for various values of K_2, when K_1=13, 20, 38. In this case, only the flutter occurs for all values of K_2. And also, the critical distributed friction force decreases at first and increases later as the spring constant K_2 increases for a fixed value of K_1.

Meanwhile, the spring stiffness $K_2 \geq 10^5$ can be considered as a rigid support since the critical distributed friction force changes little with K_2 above 10^6.

Figure 6 presents the critical distributed friction forces for various values of K_2, when K_1=39, 40, 41. The transition from a flutter to a divergence occurs as K_2 increases when K_1=39 and 40.

For K_1=41, only the divergence occurs for all K_2, and the critical distributed friction force increases as the spring constant K_1 increases for a fixed value of K_2.

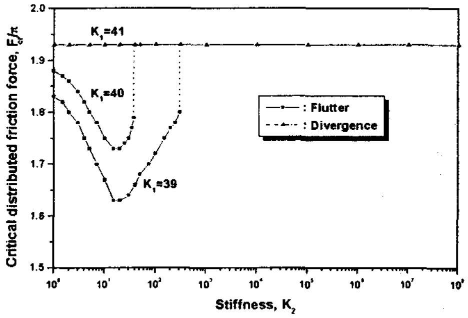

Fig. 6 Instability transitions depending on the spring stiffness (K_1 = 39, 40, 41 and K_2).

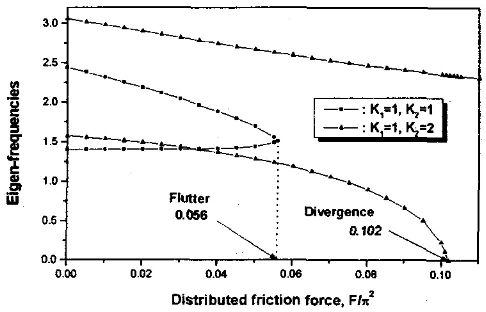

Fig. 7 Variations of eigen frequencies with spring stiffness (K_1 = 1 ; K_2 = 1 and 2).

Figure 7 shows the eigen-frequencies for various distributed friction forces when K_1=1, and K_2=1 and 2. The first and the second eigen-frequencies meet each other at the critical value of F_{cr}/π^2 =0.056 for both K_1 and K_2 equal to 1. The instability type is the flutter. However, the divergence occurs when the first eigen-frequency becomes zero at the critical value of F_{cr}/π^2=0.102 for K_1=1 and K_2=2.

Figure 8 presents the results when K_2=2 and 3 for K_1=2. The critical values of the dimensionless distributed friction force, F_{cr}/π^2, are 0.104 and 0.203.

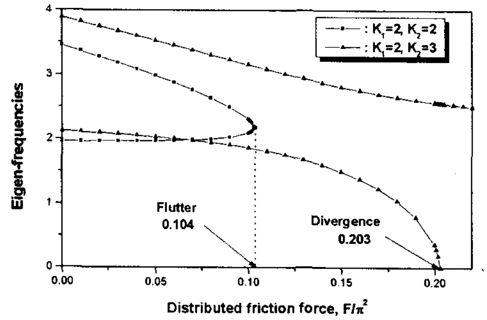

Fig. 8 Variations of eigen frequencies with spring stiffness ($K_1=2$; $K_2=2$ and 3).

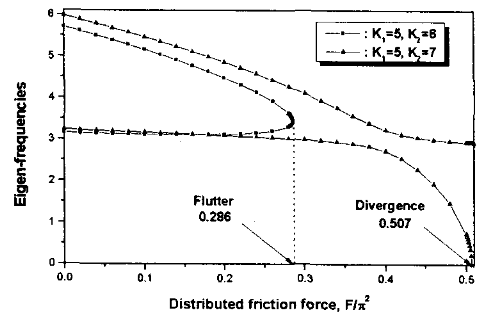

Fig. 9 Variations of eigen frequencies with spring stiffness ($K_1=5$; $K_2=6$ and 7).

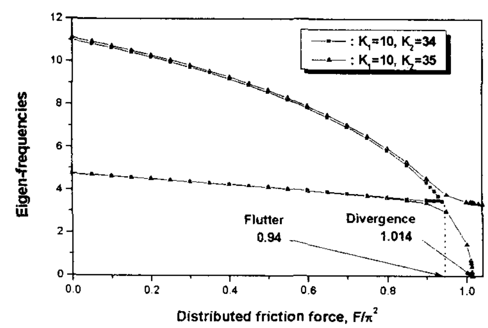

Fig. 10 Variations of eigen frequencies with spring stiffness ($K_1=10$; $K_2=34$ and 35).

Figure 9 shows the results when K_2=6 and 7 for K_1=5. The critical values of the dimensionless distributed friction force, F_{cr}/π^2, are 0.286 and 0.507.

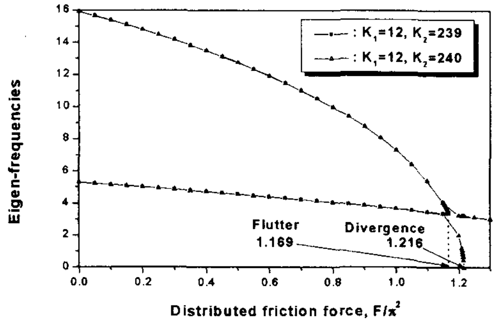

Fig. 11 Variations of eigen frequencies with spring stiffness ($K_1=12$; $K_2=239$ and 240).

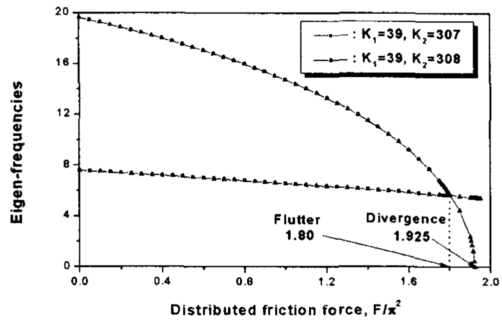

Fig. 12 Variations of eigen frequencies with spring stiffness ($K_1=39$; $K_2=307$ and 308).

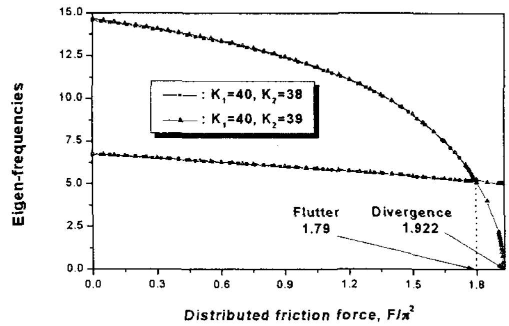

Fig. 13 Variations of eigen frequencies with spring stiffness ($K_1=40$; $K_2=38$ and 39).

Figures 10 through 13 present the transition of the instability type from a flutter to a divergence for a fixed value of K_1 as shown in figures 7 and 8. As can be seen in these figures, a slight change of K_2 has a great influence on the transition of the instability type.

4. Conclusions

The dynamic stability of a disc brake pad was investigated by assuming the system as the beam supported elastically subjected to the uniformly distributed friction forces. The following results were obtained.

1. The transition of the instability type from a flutter to a divergence occurs as K_2 increases for $K_1 \leq 12$ and $39 \leq K_1 \leq 40$. However, only the flutter occurs for all values of K_2 when $13 \leq K_1 \leq 38$. And only the divergence occurs for $K_1 \geq 41$. It is, therefore, found that the spring constant has a great influence on both the instability type and the critical distributed friction force.

2. The critical distributed follower friction force increases as the spring constant K_1 increases for a fixed value of K_2.

References

(1) Beck, M., 1952, "Die Knicklast des Einseitig Eingespannten, Tangential gedrückten Stabes", *Zeitschrift für Angewandte Mathematik und Physik(ZAMP)*, Vol.3, pp.225~228.

(2) Leipholz, H. H. E., 1972, "On the Sufficiency of the Energy Criterion for the Stability of Certain Nonconservative Systems of the Follower-Load Type", *ASME, Journal of Applied Mechanics*, Vol.39, pp.717~722.

(3) Leipholz, H. H. E., 1980, "Stability of Elastic Systems", Sijthoff & Noordhoff International Publishers.

(4) Leipholz, H. H. E., 1986, "On Principles of Stationarity for Non-selfadjoint Rod Problems", *Computer Methods in Applied Mechanics and Engineering*, Vol.59, pp.215~226.

(5) Felske, A., Hoppe, G. and Matthai, H., 1978, "Oscillations in Squealing Disk Brakes-Analysis of VibrationModes by Holographic Interferometry", *SAE Paper* No. 780333.

(6) Tan, C. A. and Kang, B., 1998, "A Study on the Root Causes of Disc Brake Squeal", *Ford Motor Company Technical Report*, No. TAN /TR-98-02.

(7) Fieldhouse, J. D. and Newcomb, P., 1993, "The Application of Holographic Interferometry to the Study of Disk Brake Noise", *SAE Paper*, No. 930805.

(8) Richmond, J. W., Kao, T. K. and Moore, M. W., 1996, "The Development of Computational Analysis Techniques for Disc Brake Pad Design", *Advances in Automotive Braking Technology* (Barton, D. C., editor), pp.69~86.

(9) Hulten, J. and Flint, J., 1999, " An Assumed Modes Method Approach to Disc Brake Squeal Analysis", *Proceedings of the SAE International Congress and Exposition*, Detroit, MI, March, Paper No. 1999-0101335.

(10) Kang, B. and Tan, C. A., 2000, "Parametric Instability of a Leipholz Column under Periodic Excitation", *Journal of Sound and Vibration*, Vol.229, pp.1097~1113.